ELASTIC FULL-WAVEFORM INVERSION OF SINGLE-COMPONENT MARINE SEISMIC DATA: PRELIMINARY RESULTS ON THE MARMOUSI-2 MODEL

R. Lo Bue, A. Tognarelli, M. Aleardi, A. Mazzotti
Earth Sciences Department, University of Pisa, Italy

Introduction. The theoretical concepts of full-waveform inversion (FWI) date back to the early 1980s (Tarantola, 1984), but due to lack of sufficient computer power, the application of FWI to seismic data did not take off until a few years ago. In particular, over the past several years, the industry has been making large strides toward using gradient-based full-waveform inversion (FWI) to build velocity models for use with pre-stack depth migration (Sajeva *et al.,* 2016; Aleardi *et al.,* 2016) after many synthetic model exercises, the attention has turned to the use of field data with the acoustic approximation of the two-way wave propagation (Morgan *et al.,* 2013). These studies have shown that if the acquired data provide long offsets and low frequencies in the range of 2 to 3 Hz, gradient-based FWI can iteratively build a high-fidelity velocity model by means of consecutive use of data with increasing frequency bandwidth (the so-called multiscale approach; Bunks *et al.,* 1995). In addition, although the acquired data are not acoustic (but more realistically viscoelastic and anisotropic) it has been demonstrated that the 3D FWI can bring significant uplift to the details in the acoustic velocity field and thus create superior migrated images.

Recent computational improvements allowed for the simulation of 3D elastic wavefields and thus undertake the challenge of elastic full-waveform inversion (EFWI). Differently from acoustic FWI that is primarily focused on inverting diving waves, EFWI has the ability to simultaneously invert reflected and transmitted energy using traveltime, amplitude, and phase information. In this context, EFWI can theoretically be an optimal tool to derive high-resolution and reliable elastic characterizations of the subsurface that are crucial in many geophysical applications, but particularly in reservoir characterization studies in which only primary P-P reflections and 1D convolutional forward models are routinely used (e.g. Aleardi and Ciabarri, 2017).

Obviously, the non-linearity and the ill-conditioning of FWI increase as many wave phenomena (multiples or converted waves) or different model parameters (*Vp, Vs*, density, viscoelastic and anisotropic parameters) are simultaneously inverted (Operto *et al.,* 2013). For this reason, applications of EFWI are primarily focused on inverting multicomponent seismic data (Sears *et al.,* 2010; Prieux *et al.,* 2013; Vigh *et al.,* 2014) that compared to conventional single-component data, bring in additional information about shear wave velocity. However, acquiring multicomponent seismic data is expensive especially in deep-water areas, where hardware limitations prevent multicomponent technology from being extended to water depths in excess of 1500 m. For this reason, in this work we assess the ability of EFWI of single-component data to provide accurate elastic subsurface models that could be used as input for reservoir characterization studies. In the following we show some preliminary results obtained on the Marmousi-2 model, which is an elastic model that reproduces a geological profile of north Quenguela in the Quanza Basin in Angola (Martin *et al*., 2006). We primarily focus our attention on the evaluation of the accuracy and quality of the *Vp*, *Vs* and corresponding *Vp*/*Vs* models. The inversion strategy, uses starting models that nicely approximate the true elastic model and moves from low frequencies to high frequencies, using both early arrivals, diving waves and reflected events. The density was kept constant to maintain the inversion at a simple level, which allowed us to draw essential conclusions.

The Marmousi-2 model and the inversion approach. The Marmousi-2 elastic model (Figs. 1a and 1b) has been developed from the Marmousi-1 acoustic model. Both models aim to reproduce the geology of the north Quenguela in the Quanza Basin in Angola. Marmousi-2 preserves the Marmousi-1 lithologies and geological structures but is deeper and laterally more extended. The sedimentary sequence is quite simple in the left and right edges of the model, but it is very complex in the centre where thrust structures, salt bodies and high-angle normal

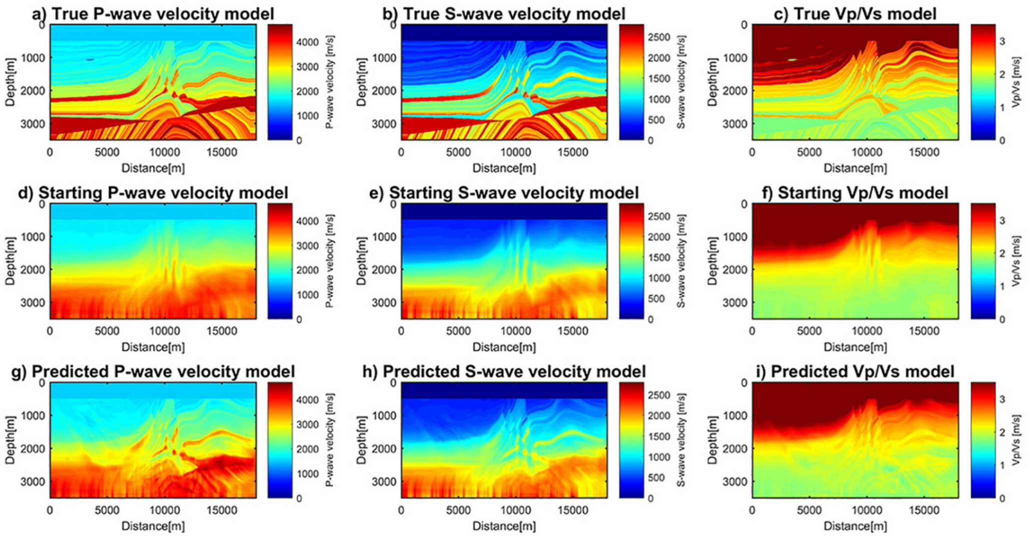

Fig. 1 - *Vp*, *Vs* and *Vp*/*Vs* of the true (a, b, c), starting (d, e, f) and final predicted (g, h, i) models.

faults are present. Differently from the Marmousi-1, some reservoir levels with different fluid saturation conditions have also been included into the Marmousi-2 model.

We employ a 2D time-domain elastic FWI code with the steepest-descent as the optimization tool and a finite difference method as forward modelling. The forward modelling code adopts absorbing boundaries to avoid artificial signal reflections at the edges of the model. In order to attenuate the risk to converge toward a local minimum of the objective function, we used the multi-scale approach. The inversion employs the standard adjoint state method to compute the gradient of the objective function that is the L2 norm misfit between observed and modelled seismic data. The modelling and the inversion grids contain 3601 grid points along the horizontal direction and 701 grid points along the vertical direction. For the computation of the synthetic observed data, we use the elastic wave equation and therefore the P-wave and S-wave velocity models, and the constant density model, were the input to the forward modelling. As the source wavelet, we employ a Ricker wavelet with 60 Hz maximum frequency and a 0.5 ms sampling interval. The acquisition geometry was defined by a towed-streamer system, composed by 181 sources (with a source interval of 50 m) and 357 receivers (with a receiver interval of 25 m) all placed in the water at a depth of 12.5 m. To make the EFWI inversion feasible, a long-offset (9 km) acquisition geometry was designed. The 5 m grid-spaced model is numerically stable and non-dispersive for the P- and S-waves velocities, and thus it ensures realistic results.

We perform several experiments varying the acquisition geometry, the number of source gathers considered in the inversion, varying the starting model and its resolution. However, for the lack of space, in the following we only show the results obtained for a single test in which we consider 90 out of 181 shot gathers. We perform 70 iterations, 5 for each of the following frequencies: 2 Hz, 3 Hz, 5 Hz, 7 Hz, 9 Hz, 11 Hz, 13 Hz, 15 Hz, 17 Hz, 20 Hz, 22 Hz, 25 Hz, 27 Hz and 30 Hz. The proper choice of the initial model is crucial for the convergence of the gradient-based FWI to the global minimum. For this reason, in the following the starting models for both *Vp* and *Vs* are directly derived from the true model by applying a moving-average filter.

Results. We now show the results obtained for a single inversion test. Figs. 1a to 1c show the true *Vp*, *Vs* and *Vp*/*Vs* models, respectively; Figs. 1d to 1f illustrate the elastic properties of the starting models, whereas Figs. 1g to 1i represent the final predicted *Vp*, *Vs* and the corresponding *Vp*/*Vs* fields, respectively. We observe that the EFWI has been able to progressively add high-frequency details to the starting *Vp* and *Vs* models. In particular, the inversion allows for a

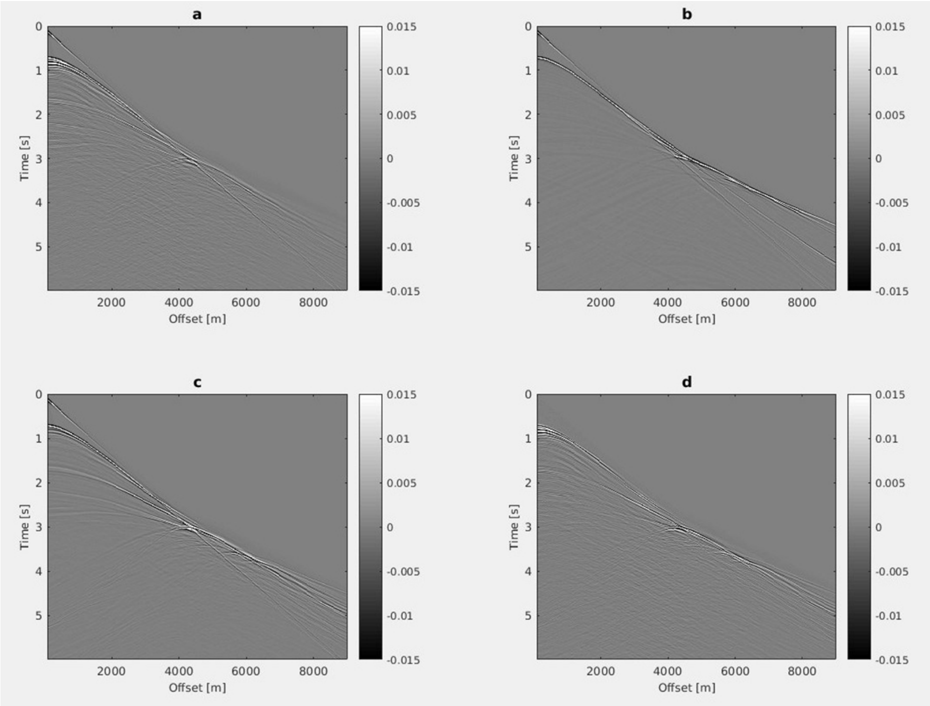

Fig. 2 - Synthetic seismic data computed on the true model (a), on the starting model (b), and on the predicted model (c). (d) Differences for a single shot gather between the observed seismic data (a) and the predicted data (c).

good reconstruction of the medium scale geological characteristics in the central part of the model, such as the thrust structures and the salt bodies. Differently, due to the poor seismic illumination, the quality of the reconstruction decreases moving toward the leftmost and deeper edges of the model, where the predicted velocities remain very similar to the starting models. At a first glance, Fig. 1i shows that the estimated *Vp*/*Vs* ratio contains some high-frequency characteristics that are not present in the starting *Vp*/*Vs* model. At the large scale of Fig. 1, seems that having realistic P- and S-wave velocity starting models, and thus a realistic *Vp*/*Vs* ratio, allows for an accurate reconstruction of the subsurface *Vp* and *Vs* fields.

Fig. 2a shows an example of observed shot gather filtered below 60 Hz. Figs. 2b to 2d show the corresponding shot computed on the starting model, on the final predicted model, and the differences between observed and the predicted shots, respectively. In Fig. 2b note that due to the long-wavelength structure, only diving waves generate on the starting model. The fair match between observed and predicted data demonstrates that the inversion actually converges toward a minimum of the misfit function. Indeed, even though some reflections are unpredicted and the correct amplitudes of the events are sometimes mispredicted, the diving waves are totally recovered and the overall energy of the waveform differences is small.

Figs. 3a and 3b offer a closer look at the final predictions that allows for a more quantitative assessment of their features. In this case the results are compared along two velocity columns of the Marmousi-2 model located at 10935 m and 15000 m from the leftmost edge of the model. We note that the estimated *Vp* model fairly reproduces the velocity variations and the velocity contrasts of the true model. Differently, the estimated *Vs* field underpredicts the velocity contrasts that characterize the true model. In other words, the estimated shear-wave velocity is mainly a low-pass filtered version of the true one. But more importantly the comparison of the estimated and the true *Vp*/*Vs* ratios, demonstrate that the EFWI has not been able to retrieve reliable estimations of this elastic parameter. In particular, if we focus our attention on

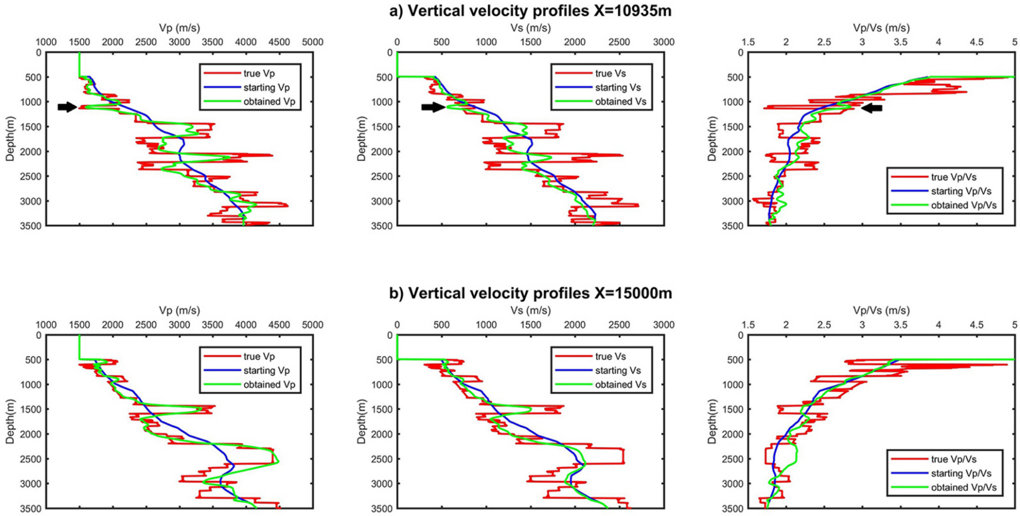

Fig. 3 - a, b) Comparison between true, starting and predicted vertical velocity profiles corresponding to two horizontal coordinates, respectively. The black arrows in (a) indicate the reservoir layer.

the reservoir interval (black arrows in Fig. 3a) we note that the inversion correctly estimates the significant decrease in *Vp* that marks the transition from the cap-rock to the reservoir layer, but fails to reproduce the corresponding increase in *Vs*. For the reservoir layer, the algorithm erroneously predicts a decrease in *Vs* and increase in *Vp*/*Vs* ratio instead of an increase in *Vs* and a corresponding strong decrease in *Vp*/*Vs* ratio. The good data reconstruction shown of Fig. 2 and the erroneous predictions of Fig. 3, indicate that the observed seismic data (marine data with single-component recording) does not contain enough information to constrain the *Vs* estimates, and for this reason, the final *Vp*/*Vs* model is not much modified from the initial to the reconstructed model. In other words, only the *Vp* information guide the inversion process. These outcomes were also confirmed by some additional FWI tests (not shown here) in which, for example, the initial P-wave models is kept fixed to the true model and only the *Vp*/*Vs* ratio is modified. Our preliminary results seem to indicate that EFWI of single-component marine seismic data, is not able to achieve reliable *Vs* and *Vp*/*Vs* estimations even if optimal starting models for both *Vs* and *Vp* are provided.

Conclusions. In this work, we demonstrated the difficulty of shear waves velocity estimations for elastic full-waveform inversion (EFWI) of single-component seismic data, even if optimal starting models for the compressional and shear waves velocities are provided. To draw essential conclusions, we kept the inversion at a simple level. In particular, we limited our attention to the inversion of synthetic data computed on the Marmousi-2 model. We adopted a time-domain FWI algorithms that makes use of a multi-scale approach and a steepest-descent optimization procedure. Our study indicates that single-component (pressure) seismic data does not provide enough information to reliably constrain *Vs* and *Vp*/*Vs* estimations in a standard EFWI approach.

Other EFWI approaches, such as target oriented or layer stripping methods, or the inclusion of multicomponent data in the observed data may help to improve the resolution and the reliability of the inversion results, which are certainly needed for reservoir characterization applications.

Therefore, the challenge remains of how to use EFWI when only pressure measurements are acquired, as it commonly happens in marine data acquisition. The next step of our research will be to compare the results provided by EFWI to those yielded by a more conventional linear amplitude versus angle inversion of P-P wave reflection coefficients.

References

Aleardi, M., and Ciabarri, F. 2017: Application of different classification methods for litho-fluid facies prediction: A case study from offshore Nile Delta. Journal of Geophysics and Engineering, 14, 1087

Aleardi, M., Tognarelli, A., and Mazzotti, A. 2016: Characterisation of shallow marine sediments using high-resolution velocity analysis and genetic-algorithm-driven 1D elastic full-waveform inversion. Near Surface Geophysics, 14(5), 449-460.

Bunks, C., Saleck, F. M., Zaleski, S., and Chavent, G. 1995: Multiscale seismic waveform inversion. Geophysics, 60(5), 1457-1473.

Martin, G. S., Wiley, R., and Marfurt, K. J. 2006: Marmousi-2: An elastic upgrade for Marmousi. The Leading Edge, 25, 156-166.

Morgan, J., Warner, M., Bell, R., Ashley, J., Barnes, D., Little, R., Roele, K., and Jones, C. 2013: Next-generation seismic experiments: wide-angle, multi-azimuth, three-dimensional, full-waveform inversion. Geophysical Journal International, 195(3), 1657-1678.

Operto, S., Gholami, Y., Prieux, V., Ribodetti, A., Brossier, R., Metivier, L., and Virieux, J. 2013: A guided tour of multiparameter full-waveform inversion with multicomponent data: From theory to practice. The Leading Edge, 32(9), 1040-1054.

Prieux, V., Brossier, R., Operto, S., and Virieux, J. 2013: Multiparameter full waveform inversion of multicomponent ocean-bottom-cable data from the Valhall field. Part 2: Imaging compressive-wave and shear-wave velocities. Geophysical Journal International, 194(3), 1665-1681.

Sajeva, A., Aleardi, M., Stucchi, E., Bienati, N., and Mazzotti, A. 2016: Estimation of acoustic macro models using a genetic full-waveform inversion: Applications to the Marmousi model. Geophysics, 81(4), R173-R184.

Sears, T. J., Barton, P. J., and Singh, S. C. 2010: Elastic full waveform inversion of multicomponent ocean-bottom cable seismic data: Application to Alba Field, UK North Sea. Geophysics, 75(6), R109-R119.

Tarantola, A. 1984: Inversion of seismic reflection data in the acoustic approximation. Geophysics, 49(8), 1259-1266.

Vigh, D., Jiao, K., Watts, D., and Sun, D. 2014: Elastic full-waveform inversion application using multicomponent measurements of seismic data collection. Geophysics, 79(2), R63-R77.